



SUDAR NO. 446

STANFORD UNIVERSITY  
CENTER FOR SYSTEMS RESEARCH

Synthesis of Hover Autopilots  
for Rotary-Wing VTOL Aircraft

by

W. E. Hall  
A. E. Bryson

CAS

*Guidance and Control Laboratory*

June 1972

Prepared under  
NASA 2-SK5 for the U. S. Army  
Air Research and Mobility Command  
Ames Directorate  
NASA Ames Research Center  
Moffett Field, California

SYNTHESIS OF HOVER AUTOPILOTS FOR ROTARY-WING VTOL AIRCRAFT

By

W. E. Hall

A. E. Bryson

SUDAAR NO. 446

June 1972

Guidance and Control Laboratory

Prepared under

NAS 2-5143 for the U. S. Army  
Air Research and Mobility Command  
Ames Directorate  
NASA-Ames Research Center  
Moffett Field, California

Department of Aeronautics and Astronautics  
Stanford University  
Stanford, California

## ABSTRACT

The synthesis of autopilots for rotary-wing VTOL (vertical takeoff and landing) aircraft is more complicated than for conventional aircraft due to the added degrees of freedom of the rotor. In previous reports (see References) we have shown that improved aircraft response to disturbances can be obtained by considering rotor dynamics when designing the autopilot. These conclusions were based on feeding back perfect information on all rotor and fuselage state variables (angles, angular velocities and translation velocities). This report considers the practical situation where imperfect information on only a few state variables is available. Filters are designed to estimate all the state variables from noisy measurements of fuselage pitch/roll angles and from noisy measurements of both fuselage and rotor pitch/roll angles. The mean square response of the vehicle to a very gusty, random wind is computed using various filter/controllers and is found to be quite satisfactory although, of course, not so good as when one has perfect information (idealized case).

The second part of the report considers precision hover over a point on the ground. A vehicle model without rotor dynamics is used and feedback signals in position and integral of position error are added. The mean square response of the vehicle to a very gusty, random wind is computed, assuming perfect information feedback, and is found to be excellent. The integral error feedback gives zero position error for a steady wind, and smaller position error for a random wind.

## TABLE OF CONTENTS

	<u>Page</u>
Abstract . . . . .	iii
Nomenclature . . . . .	vi
Illustrations and Tables . . . . .	viii
 1. SYNTHESIS OF AUTOPILOTS TO MAINTAIN NEARLY ZERO VELOCITY IN HOVER USING FUSELAGE ANGLE MEASUREMENTS WITH AND WITH- OUT ROTOR ANGLE MEASUREMENT . . . . .	 1
1.1 Introduction . . . . .	1
1.2 A Tenth Order Model of Roll-Pitch-Horizontal Velocity for a Rotary-Wing VTOL Aircraft Near Hover . . . . .	 1
1.3 A Wind Model . . . . .	3
1.4 Measurement Error Models . . . . .	5
1.5 A Filter to Estimate Vehicle States From Measurements of Fuselage Roll/Pitch Angles . . . . .	 7
1.6 A Filter to Estimate Vehicle States from Measurements of Fuselage Roll/Pitch Angles and Rotor Roll/Pitch Angles . . . . .	 9
1.7 Mean Square Response of Controlled Vehicle to a Random Wind . . . . .	 12
 2. SYNTHESIS OF AUTOPILOTS TO HOVER OVER A POINT ON THE GROUND .	 15
2.1 Introduction . . . . .	15
2.2 A Sixth Order Model of Roll-Pitch-Horizontal Velocity for a Rotary-Wing VTOL Aircraft Near Hover . . . . .	 15
2.3 Equilibrium State for Constant Wind; Feedback of Integral of Error . . . . .	 16
2.4 Integral Controller Design by Quadratic Synthesis . . . . .	18
2.5 Mean Square Response of Controlled Vehicle to a Random Wind . . . . .	 20
 APPENDIX: Determination of Feedback Gains on Wind . . . . .	 22
References . . . . .	24

# NOMENCLATURE

A	matrix of state weighting coefficients (i.e., weighting of $\theta_F = A_{\theta_F}$ )
C	matrix of control gains
F	open loop (controls fixed) dynamics matrix
G	control distribution matrix
H	measurement scaling matrix
K	matrix of Kalman filter gains
P	covariance of error estimate
Q	power spectral density of process noise
R	power spectral density of measurement noise
X	mean square response matrix of state responses
$\hat{X}$	mean square response matrix of state estimates
p	roll rate
q	pitch rate
u,v	longitudinal and lateral velocities of vehicle c.g. in vehicle axes
$\underline{u}$	control vector
x,y	longitudinal and lateral position of vehicle c.g.
$\eta$	integral of lateral position
$\theta$	pitch angle
$\theta_c$	lateral cyclic pitch
$\theta_s$	longitudinal cyclic pitch
$\xi$	integral of longitudinal position
$\tau_c$	time constant

$\phi$  roll rate  
 $\Gamma$  process noise distribution matrix

Subscripts

$( )_R$  rotor state  
 $( )_F$  fuselage state  
 $(\hat{\phantom{x}})$  estimated state  
 $(\sim)$  error in estimated state

Superscripts

$( )'$  matrix of augmented system  
 $( )^T$  matrix transpose (rows and columns interchanged)

## ILLUSTRATIONS

		<u>Page</u>
Fig. 1-1	Model Reference Axes . . . . .	2
Fig. 1-2	Block Diagram of Filter-Controller as a Dynamic Compensator . . . . .	12

## TABLES

Table 1-1	Elements of the Open-Loop Dynamics Matrix, the Control Distribution Matrix, and a Feedback Gain Matrix for a Mathematical Model of the Sikorsky S-61 Helicopter . .	4
Table 1-2	Gain Matrices for Filters A and B . . . . .	8
Table 1-3	Eigenvalues ( $\text{sec}^{-1}$ ) of Estimate Errors for Filters A and B Compared with Open-Loop and Closed-Loop Eigenvalues . . . . .	9
Table 1-4	RMS Error in Filter Estimates for Filters A and B . . .	9
Table 1-5	Gains for Filters C and D . . . . .	10
Table 1-6	Eigenvalues ( $\text{sec}^{-1}$ ) of Estimate Errors for Filters C and D . . . . .	11
Table 1-7	RMS Errors of Estimates for Filters C and D . . . . .	11
Table 1-8	Predicted RMS Responses of Vehicle to Random Wind Using Various Filter/Controllers . . . . .	14
Table 2-1	Roll-Pitch-Horizontal Velocity Model of Sikorsky S-61 Helicopter for Instantaneous Rotor Tilting . . . .	16
Table 2-2	Feedback Gains for Sikorsky S-61 Helicopter with and without Integral Error Feedback . . . . .	19
Table 2-3	Additional Gains on Wind Components with 3.2 sec Correlation Time . . . . .	19
Table 2-4	Predicted RMS Responses of Vehicle to Random Wind with and without Integral Control . . . . .	20
Table 2-5	Predicted RMS Responses of Vehicle to Random Wind with Integral Control for Various Wind Correlation Times . . . . .	21

# 1. SYNTHESIS OF AUTOPILOTS TO MAINTAIN NEARLY ZERO VELOCITY IN HOVER USING FUSELAGE ANGLE MEASUREMENTS WITH AND WITHOUT ROTOR ANGLE MEASUREMENT

## 1.1 Introduction

In a previous report [BR1], we discussed the synthesis of hover autopilots by a new, more efficient, quadratic synthesis technique. We assumed, in that work, that perfect measurements of all the vehicle states were available. In a subsequent report [BR2] we gave a detailed description of this new technique for "Optimal Control and Filter Synthesis by Eigenvector Decomposition." In this report, we use the eigenvector decomposition technique to synthesize filters to estimate the vehicle states for the tenth order system of [BR1] from measurements containing random errors. These filters are then combined with the "perfect-state-information controller" developed in [BR1] to form a dynamic compensating network. Finally, the mean-square response of the controlled vehicle to a random horizontal wind is determined.

## 1.2 A Tenth Order Model of Roll-Pitch-Horizontal Velocity for a Rotary-Wing VTOL Aircraft Near Hover

A two-rigid-body model (TRBM) of a typical rotary-wing VTOL aircraft near hover was derived in [HA1]. The fuselage is regarded as one rigid body and the spinning rotor is modeled as another (axially symmetric) rigid body that can be tilted with respect to the fuselage by the controls (longitudinal and lateral cyclic pitch)(see Fig. 1). This leads to a 16th order mathematical model since there are 3 translational degrees of freedom (DOF) for the mass center, 3 angular DOF for the fuselage, and 2 angular DOF for the rotor (assuming constant rotor spin velocity). If we disregard horizontal position of the mass center, the model reduces to 14th order; near hover, vertical motion and yaw motion are both virtually uncoupled, and the model reduces to one 10th order system and two uncoupled 2nd order systems (collective pitch controlling the vertical motion and tail rotor controlling the yaw motion).



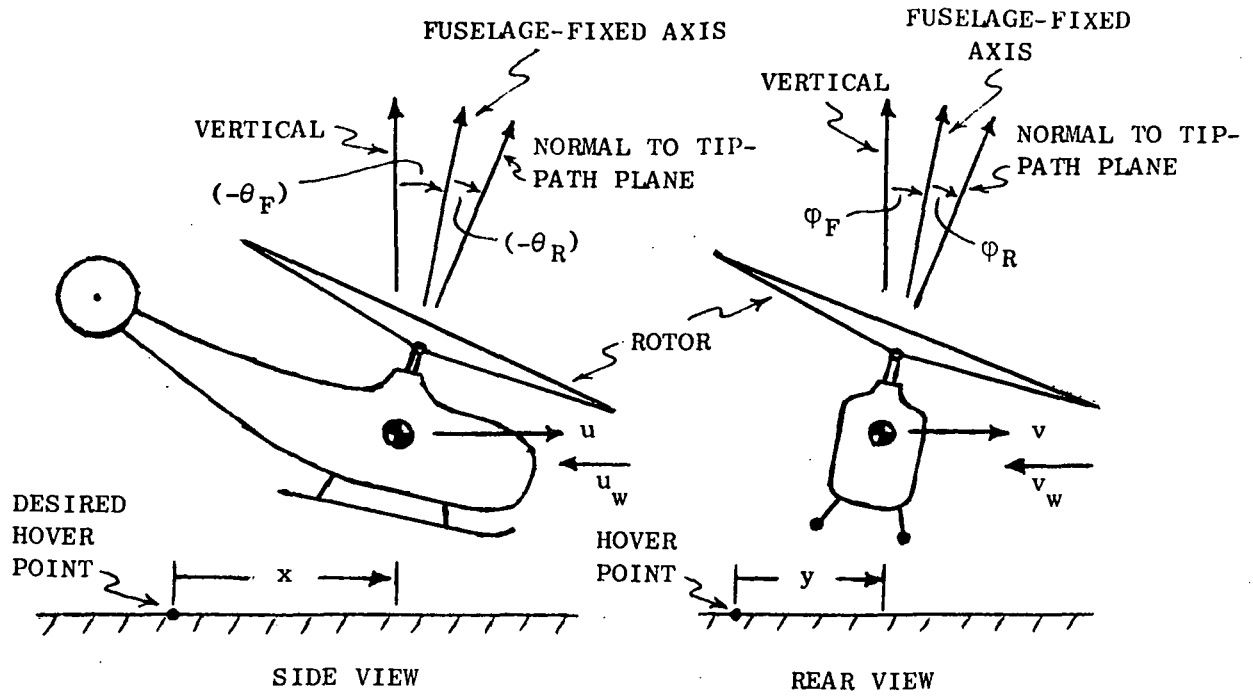


Fig. 1-1. MODEL REFERENCE AXES.

Our attention in this section, as in [BR1], is focused on the 10th order system. Using the results of many previous investigators for rotor-fuselage aerodynamic forces and torques, we constructed the following constant-coefficient linear model for the roll-pitch-horizontal translation motions (linearized about equilibrium hover):

$$\dot{\underline{x}} = \underline{F}\underline{x} + \underline{G}\underline{u} \quad (1)$$

where

$$\underline{x}^T = (\theta_R, \phi_R, q_R, p_R, \theta_F, \phi_F, q_F, p_F, u, v) = \text{state vector},$$

$$\underline{u}^T = (\theta_c, \theta_s) = \text{control vector},$$

and

$$q_R = \dot{\theta}_R, \quad p_R = \dot{\phi}_R, \quad q_F = \dot{\theta}_F, \quad p_F = \dot{\phi}_F.$$

(u,v) are velocity components of the mass center along the (x,y) fuselage axes.  $(\theta_s, \theta_c)$  are longitudinal and lateral cyclic pitch perturbations, respectively. A feedback controller,  $\underline{u} = C\underline{x}$ , was designed in [BR1] for this system, assuming perfect measurements of the ten vehicle state variables.

In Table 1, the elements of the  $10 \times 10$  matrix  $F$ , the  $10 \times 2$  matrix  $G$ , and the  $2 \times 10$  matrix  $C$ , are given for the Sikorsky S-61 helicopter. For controls fixed ( $\theta_s = \theta_c = 0$ ), the characteristic roots of this model are quite close to those of a model used by Sikorsky engineers (see [BR1]).

### 1.3 A Wind Model

The wind components  $(u_w, v_w)$  along the (x,y) fuselage axes are modeled by independent exponentially-correlated Gauss-Markov processes (cf. M11). We took the components of the wind  $(u_w$  and  $v_w)$  to be independent Gauss-Markov processes defined by:

$$\begin{aligned}\dot{u}_w &= -\frac{1}{\tau_c} u_w + q_u \\ \dot{v}_w &= -\frac{1}{\tau_c} v_w + q_v\end{aligned}\tag{2}$$

where

$$E[q_u] = E[q_v] = 0, \quad E \begin{bmatrix} q_u(t)q_u(t'), & q_u(t)q_v(t') \\ q_v(t)q_u(t'), & q_v(t)q_v(t') \end{bmatrix} = \begin{bmatrix} Q_w & 0 \\ 0 & Q_w \end{bmatrix} \delta(t-t')$$

and

$$Q_w = \frac{2\sigma_w^2}{\tau_c};$$

$\tau_c$  is the correlation time of the wind. In the statistical steady state Eq. (2) gives  $E[u_w] = E[v_w] = 0$ ,  $E[u_w^2] = E[v_w^2] = \sigma_w^2$ ,  $E[u_w v_w] = 0$ . For the simulations here, we took  $\tau_c = 3.2$  sec and  $\sigma_w = 20$  ft  $\text{sec}^{-1}$ , which is a very strong, gusty wind.

Table 1-1 - Elements of the Open-Loop Dynamics Matrix, the Control Distribution Matrix, and a Feedback Gain Matrix for a Mathematical Model of the Sikorsky S-61 Helicopter

$$\begin{aligned} \dot{\underline{x}} &= \underline{F}\underline{x} + \underline{G}\underline{u} ; \quad \underline{x}^T = [\theta_R, \phi_R, q_R, p_R, \theta_F, \phi_F, q_F, p_F, u, v] \\ \underline{u} &= \underline{C}\underline{x} \quad ; \quad \underline{u}^T = [\theta_c, \theta_s] = \text{lateral, longitudinal cyclic pitch} \\ \theta &= \text{pitch angle, } \phi = \text{roll angle, } ( )_F = \text{fuselage, } ( )_R = \text{rotor} \\ u, v &\text{ are longitudinal, lateral velocity components} \\ \text{All units in feet, seconds; angles in radians.} \end{aligned}$$

$$F = \begin{bmatrix} 0 & 0 & 1 & 0 & 0 & 0 & 0 & 0 & 0 & 0 \\ 0 & 0 & 0 & 1 & 0 & 0 & 0 & 0 & 0 & 0 \\ -41.3 & -601 & -30.2 & -42.6 & 0 & 0 & -30.4 & -50.1 & .126 & -.284 \\ 599 & -56.7 & 42.6 & -29.4 & 0 & 0 & 50.2 & -30.2 & -.283 & -.122 \\ 0 & 0 & 0 & 0 & 0 & 0 & 1 & 0 & 0 & 0 \\ 0 & 0 & 0 & 0 & 0 & 0 & 0 & 1 & 0 & 0 \\ 4.97 & -.94 & -.044 & .0034 & 0 & 0 & -.0521 & .0281 & .00124 & -.00020 \\ 3.53 & 18.7 & -.013 & -.166 & 0 & 0 & -.105 & -.196 & -.00076 & -.00467 \\ -15.0 & 21.9 & 1.03 & -.045 & -32.2 & 0 & 4.37 & 1.44 & -.0166 & .0072 \\ 21.9 & 15.0 & -.045 & -1.03 & 0 & 32.2 & 1.44 & -4.37 & -.0072 & -.0166 \end{bmatrix}$$

$$G^T = \begin{bmatrix} 0 & 0 & -601 & 5.52 & 0 & 0 & -.938 & -4.97 & 21.8 & -16.8 \\ 0 & 0 & -1.47 & -599 & 0 & 0 & 1.32 & -3.52 & -16.8 & -21.8 \end{bmatrix}$$

$$C = \begin{bmatrix} .26 & , & .31 & , & .007 & , & -.001 & , & .27 & , & .97 & , & .112 & , & .272 & , & .000083 & , & -.000058 \\ -.16 & , & .17 & , & .001 & , & .004 & , & -.97 & , & .27 & , & -.535 & , & .041 & , & -.000031 & , & -.000079 \end{bmatrix}^*$$

\*These gains correspond to the performance index,  $J = \frac{1}{2} \int_0^\infty (\theta_F^2 + \phi_F^2 + \theta_s^2 + \theta_c^2) dt$ .

Equation (2) is called a "shaping filter" for the wind; using this approach,  $u_w$  and  $v_w$  become additional (eleventh and twelfth) state variables of the system. They enter into Eqs. (1) only through the aerodynamic terms where  $u$  is replaced by  $u + u_w$  and  $v$  is replaced by  $v + v_w$ . The augmented equations are then:

$$\underbrace{\begin{bmatrix} \dot{\underline{x}} \\ \dot{u}_w \\ \dot{v}_w \end{bmatrix}}_{\dot{\underline{x}}'} = \underbrace{\begin{bmatrix} F & f_u & f_v \\ 0 & -1/\tau_c & 0 \\ 0 & 0 & -1/\tau_c \end{bmatrix}}_{F'} \underbrace{\begin{bmatrix} \underline{x} \\ u_w \\ v_w \end{bmatrix}}_{\underline{x}'} + \underbrace{\begin{bmatrix} G \\ 0 \\ 0 \end{bmatrix}}_{G'} \underline{u} + \underbrace{\begin{bmatrix} 0 \\ 1 & 0 \\ 0 & 1 \end{bmatrix}}_{\Gamma} \underline{q}_w \quad (3)$$

where  $f_u = F_{i,9}$ ,  $f_v = F_{i,10}$ ,  $(i = 1, \dots, 10)$ .

The perfect-information-controller now contains four additional feedback gains on  $u_w$  and  $v_w$ :

$$\begin{bmatrix} \theta_c \\ \theta_s \end{bmatrix} = C \underline{x} + C_w \begin{bmatrix} u_w \\ v_w \end{bmatrix}. \quad (4)$$

The other twenty gains,  $C$ , are not changed by addition of these two state variables, since Eq. (2) is coupled only one-way to Eq. (1). In fact, the four additional gains,  $C_w$ , may be determined in terms of  $\tau_c$  and the steady state Riccati matrix corresponding to Eq. (1), which is shown in Appendix A. For the numerical values used here, the four additional gains are:

$$C_w = \begin{bmatrix} .00021 & , & -.00051 \\ -.00050 & , & -.00020 \end{bmatrix}. \quad (5)$$

#### 1.4 Measurement Error Models

Measurements of fuselage roll angle,  $\phi_F$ , and fuselage pitch angle,  $\theta_F$ , have been used for some time as basic inputs to autopilots. They are readily obtained from the vertical reference system of the aircraft which usually consists of a two-degree-of-freedom gyro with two electrolytic bubble levels. We have assumed that these measurements contain additive white noise with zero mean. For one system we assumed

a power spectral density of  $2.8 \times 10^{-6} \text{ rad}^2 \text{ sec}$ , which was estimated by considering an RMS error of  $.22^\circ$  with a correlation time of 0.1 second. For another, more accurate, system, we assumed an RMS error of  $.09^\circ$ , still with a correlation time of 0.1 second. Actually, vertical gyro measurements are sensitive to lateral accelerations since the bubble levels measure the "apparent vertical." Thus our white noise error model is really more appropriate to angle measurements from an inertial measurement unit (IMU) with a stable platform.

Measurements of the roll angle,  $\phi_R$ , and the pitch angle,  $\theta_R$ , of the rotor tip-path-plane are more difficult and more expensive. Direct rotor angle measurements for articulated rotors have been made with potentiometers or strain gauges on the blade flapping hinge. The principal drawback of this technique is the required resolution of the measurements from rotating to non-rotating axes. This complexity and the extra weight are justified only for flight tests and not for operational use. Other direct methods could be based on directly linking the blade tips to a shaft mounted sensor or on electromagnetic (possibly optical) techniques. For example, small electromagnetic radiators at the rotor tips could be detected at the hub by direction-sensitive receivers, two in pitch and two in roll.

Indirect rotor angle measurements have been made by sensing hub moments. The AH-56 helicopter originally used a shaft mounted gyro which was torqued by moments proportional to the hingeless blade flapping. The difficulties of this system lie in the added complexity, the poor drag characteristics of the gyro assembly, and in the problem of isolating the moment sensors from vibrations.

We have assumed that measurements of  $\phi_R$  and  $\theta_R$  contain additive white noise with zero mean, and we have considered two levels of power spectral density. One of these levels is high ( $7.1 \times 10^{-6} \text{ rad}^2 \text{ sec}$ ), corresponding to inaccurate measurements, and the other is low ( $7.1 \times 10^{-8} \text{ rad}^2 \text{ sec}$ ), corresponding to very accurate measurements. These levels were estimated by considering a correlation time of 0.1 second and RMS errors of 1.0 deg and 0.1 deg, respectively. The latter is probably

more accurate than can be expected but serves to tell us whether or not an attempt to develop very accurate measurements would be worthwhile in terms of improving vehicle response.

We did not consider the use of measurements of the fuselage angular velocities,  $p_F$  and  $q_F$ . They are easily obtained with rate gyros but would have to be supplemented either with angle measurements  $(\phi_F, \theta_F)$  or velocity measurements. Measurements of fuselage velocity  $(u, v)$  could be obtained directly from a Doppler system or indirectly from an IMU. Airspeed measurements are not very accurate at the low velocities corresponding to hover and, of course, are not measurements of ground speed but speed with respect to the air. The combination of velocity measurements from a Doppler system with rate gyro measurements would be an interesting one to consider.

#### 1.5 A Filter to Estimate Vehicle States From Measurements of Fuselage Roll/Pitch Angles

Two steady-state Kalman filters corresponding to the twelfth order model of Eq. (3) were designed using the eigenvector decomposition technique of [BR2] for measurements of  $\theta_F$  and  $\phi_F$ , assumed to contain additive white noise. Numerical values for  $F'$  were obtained from Table 1 and below Eq. (2); two values for the power spectral density of the measurement noise were used,  $2.8 \times 10^{-6} \text{ rad}^2 \text{ sec}$  for Filter A, and  $.48 \times 10^{-6} \text{ rad}^2 \text{ sec}$  for Filter B. The filters have the form

$$\dot{\hat{\underline{x}}'} = F' \hat{\underline{x}}' + G' \underline{u} + K(z - H \hat{\underline{x}}') \quad (6)$$

where

$$z = \begin{bmatrix} \theta_F + \text{noise} \\ \phi_F + \text{noise} \end{bmatrix} = \text{measurements}, \quad H = \begin{bmatrix} 0 & 0 & 0 & 0 & 1 & 0 & 0 & 0 & 0 & 0 & 0 & 0 \\ 0 & 0 & 0 & 0 & 0 & 1 & 0 & 0 & 0 & 0 & 0 & 0 \end{bmatrix},$$

$$(\hat{\underline{x}}')^T = [\hat{\theta}_R, \hat{\phi}_R, \hat{q}_R, \hat{p}_R, \hat{\theta}_F, \hat{\phi}_F, \hat{q}_F, \hat{p}_F, \hat{u}, \hat{v}, \hat{u}_w, \hat{v}_w] = \text{estimates of the state variables.}$$

The gains,  $K$ , are given in Table 2, the eigenvalues of the filter estimates,  $\tilde{x}' = (\hat{x}' - x')$  are given in Table 3, and the RMS errors in the filter estimates are given in Table 4.

Some of the gains change sign in going from Filter A to Filter B. Such sign changes with measurement accuracy are not uncommon.

The eigenvalues of the filter error, Table 3, indicate the response decay of the error relative to the uncontrolled and controlled modes of the vehicle. The smallest eigenvalues are real and indicate rather slow error decay for that filter mode.

The RMS values of the estimate errors are given in Table 4. These are the square roots of the diagonal terms of the error covariance matrix. The effect of these errors on the vehicle response is discussed in Section 1.7. The rotor estimate errors and the wind velocity errors are not significantly changed by increased fuselage measurement accuracy, but the fuselage estimate errors are substantially reduced.

Table 1-2.- Gain Matrices for Filters A and B  
(All units in seconds, feet;  
angles in radians)

Filter A - Less Accurate Measurements												
$K^T =$	2.58	.12	-3.02	-.80	5.75	.10	16.90	.22	-86.1	5.35	7550.	1320.
	.37	1.47	1.80	-6.54	.10	8.44	1.15	35.60	2.89	37.10	1430.	-8060.
Filter B - More Accurate Measurements												
$K^T =$	7.60	.71	-7.40	-2.08	8.0	.20	32.2	2.0	-172.	3.56	19450.	3360.
	.19	5.36	3.30	-17.8	.20	11.92	1.91	71.3	-2.82	89.4	3510.	-20500.

Table 1-3 - Eigenvalues ( $\text{sec}^{-1}$ ) of Estimate Errors for Filters A and B Compared with Open-Loop and Closed-Loop Eigenvalues						
Open-Loop	$-14.1 \pm 38.2j$	$-13.2 \pm 5.2j$	$-1.20 \pm .21j$	$+1.11 \pm .36j$	$+0.04 \pm .50j$	$-.31^\dagger$
*Closed-Loop	$-14.1 \pm 38.2j$	$-13.2 \pm 5.2j$	$-3.60 \pm 3.40j$	$-1.85 \pm 1.83j$	$-.02 \pm .0005j$	$-.31^\dagger$
Filter A	$-14.1 \pm 38.2j$	$-13.3 \pm 5.2j$	$-2.54 \pm 4.35j$	$-1.62 \pm 2.83j$	$-5.05, -3.40$	$-.0011^\dagger$
Filter B	$-14.1 \pm 38.2j$	$-13.3 \pm 5.2j$	$-3.49 \pm 5.90j$	$-2.13 \pm 3.82j$	$-6.65, -4.62$	$-.00044^\dagger$
*Closed-loop means with feedback gains of Table 1 on "perfect" state measurements.						
$^\dagger$ Double roots.						

Table 1-4 - RMS Error in Filter Estimates for Filters A and B (Units in seconds, feet; angles in degrees)												
	$\tilde{\theta}_R$	$\tilde{\phi}_R$	$\tilde{q}_R$	$\tilde{p}_R$	$\tilde{\theta}_F$	$\tilde{\phi}_F$	$\tilde{q}_F$	$\tilde{p}_F$	$\tilde{u}$	$\tilde{v}$	$\tilde{u}_w$	$\tilde{v}_w$
Filter A	.27	.18	1.63	1.65	.23	.28	.85	1.44	1.65	1.65	10.7	9.9
Filter B	.24	.17	1.62	1.62	.11	.14	.56	1.02	1.05	1.05	10.4	8.8

#### 1.6 A Filter to Estimate Vehicle States from Measurements of Fuselage Roll/Pitch Angles and Rotor Roll/Pitch Angles

Two other steady-state Kalman filters were designed for the model of Eq. (3); these filters have four measurements as inputs,  $\theta_R, \phi_R, \theta_F$ , and  $\phi_F$ . Both filters assumed the less accurate fuselage angle measurements (noise power spectral density  $2.8 \times 10^{-6} \text{ rad}^2 \text{ sec}$ ). Two values for the noise power spectral density of the rotor angle measurements were used,  $7.1 \times 10^{-6} \text{ rad}^2 \text{ sec}$  for Filter C, and  $7.1 \times 10^{-8} \text{ rad}^2 \text{ sec}$  for Filter D. The filters have the same form as (6) except that now



$$z = \begin{bmatrix} \theta_R + \text{noise} \\ \phi_R + \text{noise} \\ \theta_F + \text{noise} \\ \phi_F + \text{noise} \end{bmatrix} = \text{measurements}$$

$$H = \begin{bmatrix} 1 & 0 & 0 & 0 & 0 & 0 & 0 & 0 & 0 & 0 & 0 & 0 \\ 0 & 1 & 0 & 0 & 0 & 0 & 0 & 0 & 0 & 0 & 0 & 0 \\ 0 & 0 & 0 & 0 & 1 & 0 & 0 & 0 & 0 & 0 & 0 & 0 \\ 0 & 0 & 0 & 0 & 0 & 1 & 0 & 0 & 0 & 0 & 0 & 0 \end{bmatrix}.$$

The gains  $K$  are given in Table 5, the eigenvalues of the error estimates,  $\underline{\tilde{x}}' = \underline{\hat{x}}' - \underline{x}'$ , are given in Table 6, and the RMS errors of the estimates are given in Table 7.

A comparison of the RMS errors of the estimates for Filter A (Table 4) with those of Filter C (Table 7) shows only a slight reduction by adding the less accurate rotor measurements.

When the more accurate rotor measurements are used (Filter D), significant changes in the eigenvalues of the estimate errors occur (Table 6). The gains on the rotor states for this Filter D are significantly increased (Table 5). Reduction of the rotor state estimate errors is accompanied by reduction of the fuselage angle and wind velocity estimate errors, but the velocity errors are not reduced at all (Table 7).

Table 1-5 - Gains for Filters C and D  
(All units in seconds,  
feet; angles in radians)

Filter C - Less Accurate Rotor Measurements												
$K^T =$	1.99	.13	2.28	3.82	.47	.08	3.68	.17	-5.10	.86	4560.	610.
	.13	1.21	-3.42	.96	.002	.42	.28	5.90	-.07	-2.32	635.	-3160.
	1.16	.006	-1.62	-.50	4.51	.01	10.5	-.26	-66.5	3.38	3890.	704.
	.19	1.06	1.67	-5.26	.01	7.71	.54	30.2	3.91	36.2	794.	-6650.
Filter D - More Accurate Rotor Measurements												
$K^T =$	20.9	.05	218.	154.	.27	.40	10.2	2.68	119.7	-38.2	57000.	-9510.
	.05	19.8	-152.	196.	-.10	.53	-.67	34.9	-36.8	-124.	-9510.	-56500.
	.007	-.003	-.10	-.04	1.68	-.006	1.42	-.12	-33.8	.92	392.	4.32
	.001	.013	.04	-.56	-.006	3.63	.09	6.62	1.73	29.2	-75.6	-1117.

Table 1-6 - Eigenvalues ( $\text{sec}^{-1}$ ) of Estimate Errors for Filters C and D						
Filter C	$-14.2 \pm 38.2j$	$-13.2 \pm 5.6j$	$-1.78 \pm 2.42j$	$-4.58 \pm .31j$	$-.27 \pm 4.10j$	$-.0011^\dagger$
Filter D	$-15.0 \pm 41.5j$	$-22.2 \pm 1.21j$	$-12.1 \pm 10.9j$	$-1.49 \pm 1.42j$	$-.76 \pm .74j$	$-.0011^\dagger$
$^\dagger$ Double roots.						

Table 1-7 - RMS Errors of Estimates for Filters C and D (Units in feet, seconds; angles in degrees)												
	$\tilde{\theta}_R$	$\tilde{\phi}_R$	$\tilde{q}_R$	$\tilde{p}_R$	$\tilde{\theta}_F$	$\tilde{\phi}_F$	$\tilde{q}_F$	$\tilde{p}_F$	$\tilde{u}$	$\tilde{v}$	$\tilde{u}_w$	$\tilde{v}_w$
Filter C	.22	.17	1.62	1.62	.20	.27	.62	1.34	1.65	1.65	9.50	9.20
Filter D	.06	.07	1.43	1.40	.13	.19	.12	.44	1.65	1.65	4.95	5.10

### 1.7 Mean Square Response of Controlled Vehicle to a Random Wind

Combining any one of the filters of Tables 2 or 5 with the feedback gains of the perfect information controller of Table 1, produces a dynamic compensator, shown schematically below:

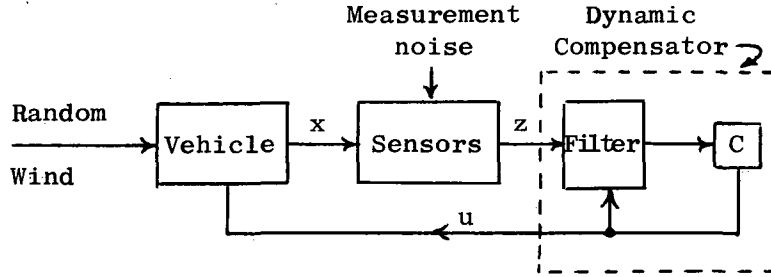


Fig. 1-2. BLOCK DIAGRAM OF FILTER-CONTROLLER-AS A DYNAMIC COMPENSATOR

$x$  = augmented state vector  
 $z$  = measurement signal  
 $u$  = control signal

The steady-state, mean-square response of the vehicle,  $X = E(xx^T)$ , using such an autopilot can be predicted by solving a set of 66 =  $\frac{1}{2}(11)$ . (12) linear equations for the elements of  $\hat{X} = E(\hat{x}\hat{x}^T)$  and adding this matrix to  $P = E(\hat{x}-x)(\hat{x}-x)^T$ ,\* i.e.,

$$X = \hat{X} + P \quad (7)$$

where

$$(F-GC)\hat{X} + \hat{X}(F-GC)^T = -KRK^T \quad (8)$$

and  $F$  is the augmented (11x11) open-loop dynamics matrix,  $G$  is the augmented (11x2) control distribution matrix,  $C$  is the augmented (2x11) feedback gain matrix,  $K$  is the augmented filter gain matrix (11x2 or 11x4),  $R$  is the measurement error power spectral density matrix  $= E(z-Hx)(z-Hx)^T$ , and  $P$  is the covariance matrix of the estimate error. In addition, the steady-state mean-square control activity can be predicted from

$$E(uu^T) = C\hat{X}C^T. \quad (9)$$

These computations were done using the OPTSYS computer program described in [BR2] and the root-mean-square (RMS) responses of the ten

\*See, e.g., [BR3], pp. 416-418.

vehicle states and the two controls\* are shown in Table 8 for autopilots using Filters A, B, C, and D. For comparison the RMS responses of the perfect information controller are also shown in Table 8; in this latter case, we assume perfect measurements of all twelve state variables; and the mean square response is obtained from

$$(F-GC)X + X(F-GC) = -\Gamma Q_w \Gamma^T \quad (11)$$

$$E(uu^T) = CXC^T \quad (12)$$

where  $\Gamma$  is defined in Eq. (3), and  $Q_w$  = power spectral density of  $q_w$ , defined in Eq. (2).

As expected, the RMS responses are smallest when perfect information on all states is fed back; however, this is an idealized situation we can never realize. Using Filter A in the autopilot (the less accurate measurements of fuselage roll/pitch angles) still produces surprisingly small responses to such a strong, gusty lateral wind.

Using Filter B in the autopilot (the more accurate measurements of fuselage roll/pitch angles) shows some reduction in RMS responses over the use of Filter A, as expected. The interesting point is that this system is better than the system using Filter C which uses the less accurate measurements of both fuselage and rotor roll/pitch angles. In other words, Filter B estimates the rotor states more accurately than they are measured for Filter C!

Filter D uses limiting, almost unattainably accurate measurements of rotor pitch and roll angles along with the less accurate measurements of fuselage pitch and roll angles. Using Filter D in the autopilot produces a substantial improvement in RMS response over the use of Filter A.

---

\*These are the square roots of the diagonal elements of  $X$  and  $E(uu^T)$ .

Table 1-8 - Predicted RMS Responses of Vehicle to  
Random Wind Using Various Filter/Controllers  
(Units in feet, seconds; angles in degrees)

	$\theta_R$	$\varphi_R$	$q_R$	$p_R$	$\theta_F$	$\varphi_F$	$q_F$	$p_F$	u	v	$\theta_c$	$\theta_s$
Filter A	.69	.59	7.21	7.62	.71	.73	1.28	2.30	3.15	2.69	.89	.95
Filter B	.54	.47	5.79	6.10	.47	.48	.85	1.71	2.35	2.01	.80	.84
Filter C	.53	.53	6.06	6.78	.55	.66	.85	2.13	2.67	2.56	.85	.84
Filter D	.19	.22	3.19	3.49	.20	.29	.21	.85	1.91	1.96	.68	.65
Perfect Info.	.08	.08	.16	.19	.05	.05	.04	.04	.84	.82	.65	.65
<p>Filter A - Less accurate fuselage measurements.  Filter B - More accurate fuselage measurements.  Filter C - Less accurate fuselage measurements and less accurate rotor measurements.  Filter D - Less accurate fuselage measurements and more accurate rotor measurements.  Perfect Info. - Perfect measurements of all states (limiting, unrealistic case).  RMS longitudinal and lateral winds 20 ft.sec.<sup>-1</sup> with 3.2 sec. correlation time.</p>												

## 2. SYNTHESIS OF AUTOPILOTS TO HOVER OVER A POINT ON THE GROUND

### 2.1 Introduction

In Part 1, the object of the controller was to keep the vehicle erect (roll and pitch angles small) and keep the rotor tilt angles small. In this part of the report, we design controllers that go further and keep the vehicle close to a specific point on the ground (longitudinal and lateral displacements small) in the presence of a random wind. A well known controller design technique for constant (but unknown) input disturbances is "integral control"; we combine this technique here with quadratic synthesis, and show that it is also useful when the input disturbances (wind in this case) are exponentially-correlated random processes.

### 2.2 A Sixth Order Model of Roll-Pitch-Horizontal Velocity for a Rotary-Wing VTOL Aircraft Near Hover

The controller designs here are based on a sixth order roll-pitch-horizontal velocity model of [BR1], which treats rotor-tilting as instantaneous. Table 1 gives the  $6 \times 6$  open-loop dynamics matrix, the  $6 \times 2$  control-distribution matrix, and the open-loop eigenvalues of the model.

This model will be augmented here by four more states  $x, y, \xi, \eta$  defined by

$$\begin{aligned}\dot{x} &= u, & \dot{\xi} &= x, \\ \dot{y} &= v, & \dot{\eta} &= y,\end{aligned}\tag{1}$$

where  $(x, y)$  are longitudinal and lateral displacements of vehicle mass center from a specified hover point on the ground, and  $(\xi, \eta)$  are integrals of these displacements.

As in Part 1, first-order shaping filters are used to simulate independent random wind components, which raises the system order to 8.

Table 2-1 - Roll-Pitch-Horizontal Velocity Model of Sikorsky S-61 Helicopter for Instantaneous Rotor Tilting

$\theta_F$  = fuselage pitch angle,  $\phi_F$  = fuselage roll angle;  $(u,v)$  = (longitudinal, lateral) velocity components;  $(\theta_c, \theta_s)$  = (lateral, longitudinal) cyclic pitch  $\equiv (-\phi_R, \theta_R) = (-\text{roll}, \text{pitch})$  tilt angles of rotor. All units in feet, seconds; angles in radians.

$$\frac{d}{dt} \begin{bmatrix} \theta_F \\ \phi_F \\ q_F \\ p_F \\ u \\ v \end{bmatrix} = \begin{bmatrix} 0 & 0 & 1 & 0 & 0 & 0 \\ 0 & 0 & 0 & 1 & 0 & 0 \\ 0 & 0 & -.415 & .318 & .00338 & .00116 \\ 0 & 0 & -1.23 & -1.58 & .00415 & -.0124 \\ -32.2 & 0 & 4.70 & -1.02 & -.0198 & -.0059 \\ 0 & 32.2 & -1.02 & -4.70 & .0059 & -.0198 \end{bmatrix} \begin{bmatrix} \theta_F \\ \phi_F \\ q_F \\ p_F \\ u+u_w \\ v+v_w \end{bmatrix} + \begin{bmatrix} 0 & 0 \\ 0 & 0 \\ -.295 & 6.27 \\ -23.1 & -1.08 \\ .977 & -32.2 \\ -32.2 & -.977 \end{bmatrix} \begin{bmatrix} \theta_c \\ \theta_s \end{bmatrix}$$

Open Loop Eigenvalues are:  $(-1.2, -1.1, .11 \pm .36j, .04 \pm .50j) \text{sec}^{-1}$ .

### 2.3 Equilibrium State for Constant Wind; Feedback of Integral of Error

For constant wind ( $u_w = \text{constant}$ ,  $v_w = \text{constant}$ ) and constant control deflections  $(\theta_c$  and  $\theta_s)$ , the vehicle has an equilibrium state with constant values of  $\theta_F, \phi_F, u$ , and  $v$ , determined by the last four equations of Table 1 with  $\ddot{\theta}_F = \ddot{\phi}_F = \dot{\theta}_F = \dot{\phi}_F = \dot{u} = \dot{v} = 0$ . There are particular values of  $\theta_c$  and  $\theta_s$  that produce  $u = v = 0$ , namely

$$\begin{bmatrix} \theta_c \\ \theta_s \end{bmatrix} = \begin{bmatrix} .00021, -.00053 \\ -.00053, -.00021 \end{bmatrix} \begin{bmatrix} u_w \\ v_w \end{bmatrix} \quad (2)$$

which correspond also to particular values of  $\theta_F$  and  $\phi_F$ :

$$\begin{bmatrix} \theta_F \\ \phi_F \end{bmatrix} = \begin{bmatrix} -.000059, .000018 \\ .000016, .000056 \end{bmatrix} \begin{bmatrix} u_w \\ v_w \end{bmatrix} \quad (3)$$

Hence, if  $u_w$  and  $v_w$  were known, additional feedback terms proportional to  $u_w$  and  $v_w$  could, in principle, bring the vehicle to equilibrium with  $u = v = 0$ .

However, such a feedback scheme is not practical for a steady wind

since it is very sensitive to knowledge of  $u_w, v_w$  and the elements of  $F, G$ , and  $C$ . Small changes (or inaccuracies) in any of these quantities would produce a steady-state with  $u$  and  $v$  constant but not equal to zero. A well-known remedy for this situation is the addition of feedback proportional to the integral of the errors (in this case  $u$  and  $v$ ). It is also quite natural in this case since the integral of velocity error is position, i.e.,

$$\begin{aligned}\dot{x} &= u, \\ \dot{y} &= v.\end{aligned}\tag{4}$$

[Note position  $(x,y)$  does not have to be measured to utilize this idea; the measured velocity components can be integrated and these "integrated errors" fed back. Of course, it is the measured velocity that is brought to zero in this case, not the true velocity.] Now, in equilibrium,  $\dot{x} = \dot{y} = 0 \Rightarrow u = v = 0$ , and the equilibrium values of the six quantities  $(\theta_F, \phi_F, x, y, \theta_c, \theta_s)$  are determined by the last four equations in Table 1 and the two feedback relations:

$$\begin{bmatrix} \theta_c \\ \theta_s \end{bmatrix} = \begin{bmatrix} C_{c\theta} & C_{c\phi} & \dots & C_{cx} & C_{cy} \\ C_{s\theta} & C_{s\phi} & \dots & C_{sx} & C_{sy} \end{bmatrix} \begin{bmatrix} \theta_F \\ \phi_F \\ 0 \\ 0 \\ 0 \\ 0 \\ x \\ y \end{bmatrix}\tag{5}$$

Thus, a "hang-off error" in  $(u,v)$  has been eliminated and there is no sensitivity to small changes (or inaccuracies) in  $u_w, v_w$ , and elements of  $F, G$ , and  $C$ .

Obviously, the same idea can be used again to eliminate the hang-off error in  $(x,y)$  if this is deemed necessary. We simply add two more states  $(\xi, \eta)$  defined by



$$\dot{\xi} = x, \quad \dot{\eta} = y$$

and feedback  $(\xi, \eta)$  with four additional feedback gains  $C_{c\xi}, C_{c\eta}, C_{s\xi}, C_{s\eta}$ . In this case  $(x, y)$  have to be measured. As long as the twenty gains in the feedback gain matrix  $C$  are chosen so that the tenth order system is stable, the vehicle will come to equilibrium with  $x = y = u = v = 0$  for a constant wind, with no sensitivity to small changes in  $u_w, v_w, F, G$ , or  $C$ .

## 2.4 Integral Controller Design by Quadratic Synthesis

The OPTSYS computer program was used to determine feedback gains for three models of the Sikorsky S-61 helicopter with and without integral error feedback. Model A is the model of Table 1 with six states  $(\theta_F, \phi_F, \dot{\theta}_F, \dot{\phi}_F, u, v)$ . Model B is the same as A with the addition of position states  $(x, y)$  where  $\dot{x} = u$ ,  $\dot{y} = v$ . Model C is the same as B with the addition of integral position states  $(\xi, \eta)$  where  $\dot{\xi} = x$ ,  $\dot{\eta} = y$ .

Table 2 gives the feedback gains obtained by using the following quadratic performance indices:

$$\text{Model A: } J = \frac{1}{2} \int_0^{\infty} (\theta_F^2 + \phi_F^2 + \dot{\theta}_F^2 + \dot{\phi}_F^2) dt$$

$$\text{Model B: } J = \frac{1}{2} \int_0^{\infty} \left( \frac{\theta_F^2 + \phi_F^2 + \dot{\theta}_F^2 + \dot{\phi}_F^2}{\theta_o^2} + \frac{x^2 + y^2}{x_o^2} \right) dt$$

$$\text{Model C: } J = \frac{1}{2} \int_0^{\infty} \left( \frac{\theta_F^2 + \phi_F^2 + \dot{\theta}_F^2 + \dot{\phi}_F^2}{\theta_o^2} + \frac{\xi^2 + \eta^2}{\xi_o^2} \right) dt$$

where  $\theta_o = 1.0$  deg.,  $x_o = 10.0$  ft.,  $\xi_o = 50.0$  ft.sec.

When the longitudinal and lateral wind,  $u_w$  and  $v_w$ , are added as states (see Section 1.3), the gains in Table 2 are unchanged but gains on the wind are added. These are shown in Table 3 for the wind correlation time of 3.2 sec.

If a filter-compensator is used with Model C, one does not "estimate"  $(\xi, \eta)$  since these are simply integrals of the position estimates (or position measurements) (see Section 1.5).

Table 2-2 - Feedback Gains for Sikorsky S-61 Helicopter with and without Integral Error Feedback ( $\underline{u} = \bar{C}\bar{x}$ , $\underline{u}^T = [\theta_c, \theta_s]$ )	
<p><u>Model A:</u> <math>\underline{x}^T = [\theta_F, \phi_F, \dot{\theta}_F, \dot{\phi}_F, u, v]</math></p> $C = \begin{bmatrix} .16 & .99 & .024 & .234 & .00012 & -.000024 \\ -1.0 & .16 & -.50 & .011 & -.000024 & -.00012 \end{bmatrix}$	
<p><u>Model B:</u> Position States Added <math>\underline{x}^T = [\theta_F, \phi_F, \dot{\theta}_F, \dot{\phi}_F, u, v, x, y]</math></p> $C = \begin{bmatrix} .17 & 1.03 & .022 & .23 & -.00034 & .0028 & -.000028 & .00017 \\ -1.05 & .17 & -.50 & .011 & .0028 & .00035 & .00017 & .0000298 \end{bmatrix}$	
<p><u>Model C:</u> Integral Position States Added</p> $C = \begin{bmatrix} .19 & 1.16 & .013 & .23 & -.0023 & .014 & -.00053 & .0033 & -.000056 & .00035 \\ -1.28 & .19 & -.49 & .08 & .016 & -.0022 & .0033 & .00053 & .00035 & .000056 \end{bmatrix}$	

Table 2-3 - Additional Gains on Wind Components with 3.2 sec Correlation Time	
$\begin{bmatrix} \theta_c \\ \theta_s \end{bmatrix} = C_w \begin{bmatrix} u_w \\ v_w \end{bmatrix}$	
<u>Model A:</u>	$C_w = \begin{bmatrix} .00020 & , & -.00049 \\ -.00049 & , & -.00020 \end{bmatrix}$
<u>Model B:</u>	$C_w = \begin{bmatrix} .00020 & , & -.00055 \\ -.00055 & , & -.00020 \end{bmatrix}$
<u>Model C:</u>	$C_w = \begin{bmatrix} .00021 & , & -.00057 \\ -.00057 & , & -.00021 \end{bmatrix}$

## 2.5 Mean Square Response of Controlled Vehicle to a Random Wind

Using the part of the OPTSYS program described in Section 1.7, Eqs. (11) and (12), for perfect information feedback, the RMS responses of the vehicle were computed for several different controllers.

Table 4 shows the RMS vehicle responses to independent random longitudinal and lateral winds, each with RMS velocity of  $20 \text{ ft. sec.}^{-1}$  and correlation time 3.2 sec., for Models A, B, and C of Section 2.4, using the gains of Tables 2 and 3. Note the reduction in RMS position errors through the addition of integral control (Model B to Model C), with no increase in RMS control activity.

Table 5 shows the effect of wind correlation time,  $\tau_c$ , on controlled vehicle response for Model C. For  $\tau_c \ll 3.2 \text{ sec.}$ , the wind is effectively white noise but has a very small power spectral density ( $2\sigma_w^2 \tau_c$ ), so it produces only small vehicle responses. For  $\tau_c \gg 3.2 \text{ sec.}$ , the wind is effectively constant, so with the integral control  $x$  and  $y \rightarrow 0$ . The largest RMS  $(x,y)$  response occurs for  $\tau_c \cong 3.2 \text{ sec.}$ , since this is in the range of time constants of the controlled vehicle.

Table 2-4 - Predicted RMS Responses of Vehicle to Random Wind with and without Integral Control (Units in feet, seconds; angles in degrees)

	$\theta_F$	$\phi_F$	$q_F$	$p_F$	$u$	$v$	$x$	$y$	$\xi$	$\eta$	$\theta_c$	$\theta_s$
Model A	.05	.04	.03	.04	.83	.82	-	-	-	-	.64	.64
Model B	.07	.07	.01	.01	.14	.14	3.8	3.8	-	-	.65	.65
Model C	.07	.07	.04	.05	.05	.04	.18	.16	1.31	1.15	.65	.65

Model A - Feeds back  $\theta_F, \phi_F, q_F, p_F, u, v$   
 Model B - Feeds back  $\theta_F, \phi_F, q_F, p_F, u, v, x, y$   
 Model C - Feeds back  $\theta_F, \phi_F, q_F, p_F, u, v, x, y, \xi, \eta$   
 Perfect measurements of all states assumed.  
 RMS longitudinal and lateral wind  $20 \text{ ft. sec.}^{-1}$  with  
 3.2 sec. correlation time.

Table 2-5 - Predicted RMS Responses of Vehicle to Random Wind with Integral Control for Various Wind Correlation Times (Units in feet, seconds; angles in degrees)

	$\theta_F$	$\phi_F$	x	y	$\xi$	$\eta$	$\theta_s$	$\theta_c$
$\infty^*$ (steady)	-.05	.08	0	0	-19.3	-13.8	-.84	.37
32	.07	.07	.02	.02	.17	.11	.65	.65
3.2	.07	.07	.18	.16	1.3	1.2	.65	.65
.00034 (white)	.02	.02	.04	.04	.25	.25	.03	.03

Model C with perfect measurements of all states assumed.

RMS longitudinal and lateral wind 20 ft.sec.<sup>-1</sup>.

\*This case is calculated by solving the 10 linear equations  $\underline{x} = (F-GC)^{-1}\Gamma \underline{w}$  where  $\underline{w} = (u_w \ v_w)^T$ .

## APPENDIX

### Determination of Feedback Gains on Wind

The system equations with exponentially-decaying wind may be written as

$$\dot{\mathbf{x}} = \mathbf{F}\mathbf{x} + \mathbf{f}w + \mathbf{G}u$$

$$\dot{w} = -aw$$

where  $\mathbf{x}$  = system state vector ,  $w$  = wind vector ,  $u$  = control vector .  
There is only a one-way coupling since  $\dot{\mathbf{x}}$  depends on  $w$  but  $\dot{w}$  does not depend on  $\mathbf{x}$  .

If the performance index to be minimized is of the form

$$J = \frac{1}{2} \int_0^{\infty} (\mathbf{x}^T \mathbf{A} \mathbf{x} + u^T \mathbf{B} u) dt ,$$

then the Hamiltonian is

$$H = \frac{1}{2}(\mathbf{x}^T \mathbf{A} \mathbf{x} + u^T \mathbf{B} u) + \lambda^T (\mathbf{F}\mathbf{x} + \mathbf{f}w + \mathbf{G}u) + \lambda_w^T (-aw) .$$

The adjoint equations become

$$\dot{\lambda} = -\mathbf{A}\mathbf{x} - \mathbf{F}^T \lambda$$

$$\dot{\lambda}_w = -\mathbf{f}^T \lambda + a^T \lambda_w$$

and the minimizing control is given by

$$u = -\mathbf{B}^{-1} \mathbf{G}^T \lambda .$$

If we let

$$\begin{bmatrix} \lambda \\ \lambda_w \end{bmatrix} = \begin{bmatrix} \mathbf{S} & \mathbf{S}_w \\ \mathbf{S}_w^T & \sigma \end{bmatrix} \begin{bmatrix} \mathbf{x} \\ w \end{bmatrix}$$

and differentiate this expression with respect to time, it is straightforward to show that  $\mathbf{S}, \mathbf{S}_w$ , and  $\sigma$  must satisfy the following differential equations:

$$\dot{S} = -SF - F^T S - A + SGB^{-1}G^T S$$

$$\dot{S}_w = -(F - GB^{-1}G^T S)^T S_w + S_w a - Sf$$

$$\dot{\sigma} = \sigma a + a^T \sigma - f^T S_w - S_w^T f + S_w^T GB^{-1}G^T S_w .$$

The matrix Riccati equation for  $S$  is the same as if there were no wind. The equation for  $S_w$  is linear but depends on  $S$ , and the equation for  $\sigma$  is also linear but depends on  $S_w$ . The feedback law may be written as

$$u = -Cx - C_w w ,$$

where

$$C = B^{-1}G^T S , \quad C_w = B^{-1}G^T S_w ,$$

so, in principle, the gains  $C_w$ , which depend on  $S_w$ , may be calculated separately after  $C$  has been determined from  $S$ .

For the steady-state case, it is easier to use OPTSYS to compute  $C$  and  $C_w$  together by eigenvalue decomposition. Nonetheless, it is important to note that  $C$  is not changed by addition of a wind model.

## REFERENCES

- [BR1] Bryson, A. E., Chasteen, L. H., Hall, W. E., and Mohr, R. L.,  
"Studies of Control and Guidance for Rotary Wing VTOL Vehicles,"  
Stanford University, SUDAAR No. 419, March 1971.
- [BR2] Bryson, A. E., and Hall, W. E., "Optimal Control and Filter Syn-  
thesis by Eigenvector Decomposition," Stanford University, SUDAAR  
No. 436, December 1971.
- [BR3] Bryson, A. E., and Ho, Y. C., Applied Optimal Control, Xerox-  
Blaisdell, Waltham, Mass., 1969.
- [HA1] Hall, W. E., "Computational Methods for the Synthesis of Rotary-  
Wing VTOL Aircraft Control Systems," Ph.D. Dissertation, Stanford  
University, August 1971.
- [MI1] Miller, D. P., and Vinje, E. W., "Fixed Based Flight Simulator  
Studies of VTOL Aircraft Handling Qualities in Hovering and Low-  
Speed Flight," AFFDL-TR-67-152, January 1968.